

## SATELLITE APPLICATIONS AT NMC

W. Baker, E. Kalnay, D. Deaven, G. DiMego, P. Julian,  
D. Esteva, R. Reynolds, T. Yu, H.-L. Pan, C. Dey, and  
K. Campana

National Meteorological Center  
Washington, D. C. 20233

### 1. INTRODUCTION

The National Meteorological Center (NMC) has initiated a comprehensive effort to improve the use of satellite data in the global data assimilation system (GDAS) including a comprehensive quality control system and a new interactive retrieval system. This article describes the present system and the various research activities that are related to this effort.

### 2. PRESENT ANALYSIS SYSTEM

Here, we describe the way we are processing satellite data in the global data assimilation system at NMC and include results comparing physical and statistical retrievals. Our current restrictions in the use of satellite data with respect to coverage and vertical extent are summarized as follows:

1. All microwave retrievals between 20N and 20S are not used by the analysis.
2. No moisture retrievals are used anywhere in the analysis.
3. Overland retrievals at and below 100 hPa are not used by the analysis.
4. For satellite sounding pairs which are within 100 km of each other, the one whose observation time differs most from the time of the analysis is excluded from the analysis. This effects overlapping swaths near the poles.

The quality control of SATEMS is not adequate and is a serious deficiency in the NMC system. A major effort is now underway to revise the entire quality control system at NMC incorporating the ideas of Gandin (1988) on complex quality control.

## 2.1 Gross Toss Limits

The standard deviations of observation-first guess (6 h forecast) differences used in computing gross toss limits are listed in Table 1.

For SATEMS, values of  $5 * Z$ -values (left column) are used. For all others the observational increment (data-first guess)  $< n\sigma$  is checked, where  $n$  is a function of the quality mark (QM).

	QM	n
keep	0	$\infty$
passed	1	7
unchecked	2	5
suspect	3	3

The other exception to the above table is for SATOBs, where  $n$  is divided by 2, if the observed speed is less than the guess speed. In the future, we plan to test replacing the SATOB speed with the guess speed for high-level, strong winds.

## 2.2 Description of the Buddy Check

In February 1987, a modified version of the "buddy" check was implemented in the regional analysis. This version was incorporated in the global data assimilation system in May 1988. The principal change from the previous scheme is in the final decision making procedure. The approach involves adding up all of the flags for agreement (KEEP) and disagreement (TOSS) and keeping those obs with at least 2 KEEPs and excluding obs with fewer than 2 KEEPs which have more than 2 TOSSes. In the original scheme flags were set to an integer 1 when agreement or disagreement occurred. The new procedure sets the flag value equal to the forecast error correlation value (height-height autocorrelation) which is nearly 1.0 for observations close to each other and nearly 0.0 if two observations are far apart. Thus, the new procedure gives much more weight in the final decision to pairs which are close together than to those pairs which are far apart.

Other changes were incorporated to be more "heavy handed" with the satellite sounding data. In order for a satellite report to be accepted, it must have a sum of 3.0 agreement flags (KEEPS). In addition, agreement flags are not set for pairs which are of the same retrieval path because their values are assumed to be correlated and not sufficiently independent. This makes it more difficult for satellite soundings to achieve the requisite number of KEEPs.

Table 1 Standard deviation of observation minus 6 hour forecast differences for z (top) in m, u (middle) in ms-1, and v (bottom) in ms-1.

P	-90 to -10	-10 to 10	10 to 30	30 to 50	50 to 90
1000	25.4	14.7	19.4	19.7	21.6
850	25.4	15.5	16.7	19.6	19.4
700	26.8	19.3	18.7	19.7	20.8
500	33.5	25.4	25.6	23.2	25.8
400	39.2	29.6	32.4	27.2	29.9
300	47.0	40.1	42.3	34.1	36.5
250	50.6	49.4	47.3	37.4	39.2
200	53.5	55.3	56.3	41.6	42.0
150	57.3	61.4	67.4	46.7	48.3
100	69.8	78.0	80.0	55.2	59.4
70	77.7	80.0	80.0	64.2	71.8
50	90.1	80.0	80.0	78.3	88.1

P	-90 to -10	-10 to 10	10 to 30	30 to 50	50 to 90
1000	4.24	3.48	4.11	4.59	4.36
850	3.88	3.18	3.71	4.12	3.58
700	4.18	3.56	4.10	4.19	3.56
500	4.79	4.25	4.81	4.79	4.41
400	5.47	4.05	5.34	5.63	5.25
300	6.59	5.76	6.53	7.11	5.66
250	9.52	5.78	7.33	6.65	5.45
200	7.29	7.81	7.61	6.72	4.38
150	6.53	8.24	7.30	5.89	3.72
100	6.96	8.77	7.73	5.07	3.67
70	6.56	7.71	5.56	7.10	5.48
50	8.29	9.85	8.66	8.22	7.61

P	-90 to -10	-10 to 10	10 to 30	30 to 50	50 to 90
1000	4.12	3.30	3.92	4.87	4.33
850	3.69	2.76	3.43	4.29	3.59
700	4.10	3.27	3.62	3.79	3.57
500	4.61	3.52	4.20	4.57	4.41
400	5.66	4.04	4.95	5.26	5.03
300	6.83	5.26	6.05	6.39	5.50
250	7.34	5.24	6.89	6.62	5.31
200	7.02	5.77	7.64	6.21	4.28
150	6.71	5.68	7.15	4.89	3.71
100	6.37	7.07	6.23	4.07	3.58
70	5.46	4.82	5.32	4.89	5.14
50	8.00	8.26	8.63	6.71	7.41

Finally, if any type of error is encountered with a satellite sounding, all of the levels of the sounding are deleted. Table 2 contains some recent statistics on the number of SATEMS used or tossed by the analysis.

Table 2 Number of SATEMS used or tossed by the analysis.

Date		Received	Used	Tossed	%
1/7/89	12Z	1809	1631	178	9.8
1/7/89	18Z	2047	1924	123	6.0
1/8/89	00Z	2391	2165	226	9.5
1/8/89	06Z	1972	1811	161	8.2

In the future, we plan to either give less weight to swath edge profiles or delete them, and use satellite thickness data in the analysis rather than heights.

### 2.3 Recent Analysis Changes

Several analysis changes in the global data assimilation system (GDAS) were evaluated during the summer of 1988. Some of the changes were designed to improve the efficiency and structure of the computer codes. Other changes were made to update and improve the statistical quantities that are used in the optimum interpolation analysis. Forecasts from the global model have improved over the past few years due to improved physical parameterizations and increased resolution. For this reason, the observation and forecast errors that are used during the assimilation have been updated to reflect the current forecast skill of the T80 global spectral model.

The following list of modifications to the GDAS were tested and evaluated in the NMC Development Division parallel system. The complete package of changes including those to the model (see Campana *et al.*, 1989) were placed into the operational job stream on November 30, 1988 at 1200 UTC.

#### 2.3.1 Treatment of Satellite Profiles

In the operational system prior to November 30, 1988, satellite profiles of geopotential height over water were anchored at 1000 mb and those over land at 100 mb. No satellite observations were used for either anchoring analysis. This procedure produced large gradients in the analysis increments and the resulting analysis near coast lines at levels above 100 mb whenever a mismatch occurred between profiles over water and those over land. This effect has been reduced by using the anchored satellite observations over water during the anchoring analysis for those over land. In addition, satellite geopotential observations will no longer be used during the analysis at or below the anchoring level as is done currently in the operational system.

A deficiency in the NMC processing of National Environmental Satellite and Data Information Service (NESDIS) satellite derived heights which had produced a systematic warming of the layer between 300 and 100 mb in areas covered mainly by satellite observations has been corrected. A gradient of height errors had developed normal to the continental coasts in regions where the satellite data were adjacent to radiosonde reports. NESDIS provides NMC with heights at selected constant pressure levels throughout the depth of the atmosphere. However, not all mandatory pressure levels are included. To provide data at all of the mandatory levels for the analysis, NMC interpolates data to the "missing" levels. The interpolation process was biased and did not preserve the total thickness of the column between reported levels.

To alleviate this problem, the height calculation technique has been modified so that the thickness values in the deeper layers are used directly as reported by NESDIS. The thickness values at the "missing" layers are then obtained using the relative values calculated previously, but constrained to the reported total value. The modified procedure does preserve the mean thickness of the column and is, therefore, unbiased. This change alone resulted in significant improvements in both the first guess and the longer forecasts.

### 2.3.2 Updated Forecast and Observation Errors

Forecast errors in the GDAS are based upon prescribed forecast error growth rates and the normalized analysis error resulting from each analysis. Since the implementation of the T80 global spectral model, forecast errors in most NMC global products have been reduced. For this reason, the forecast error growth rates that are used in the GDAS to model forecast errors have been reduced. In addition, the capability to use different growth rates in the northern and southern hemispheres and in the tropical regions has been added to the new system. The current operational and old values are shown in Table 3.

New observation errors have been constructed by some objective criteria and statistics, and by a certain amount of subjective judgment. The latter is based upon the performance of the current GDAS and the observation errors carried presently by the United Kingdom Meteorological Office (UKMO) and the European Centre for Medium Range Weather Forecasts (ECMWF). The current operational and the new values of observation error are shown in Table 4.

The estimates of radiosonde geopotential height and wind observation errors have been constructed from a study of observation minus 6-hour forecast values for radiosonde stations during the winter of 1986-87. These quantities represent the total forecast error variance including the true error of the forecast model and the errors associated with the observations. Therefore, the minimum value of the

TABLE 3 Extratropical height forecast error growth rates (top) in m and tropical values of height (m) and wind forecast error (bottom) in  $\text{ms}^{-1}$ .

LEVEL	GROWTH RATE NH		GROWTH RATE SH NEW	MAXIMUM VALUE	
	OLD	NEW		OLD	NEW
1000	5.0	3.6	4.3	40	42
850	6.3	3.8	6.2	46	38
700	8.8	4.0	6.5	54	39
500	12.5	5.5	9.3	73	50
400	16.3	6.4	12.0	87	62
300	20.0	9.5	13.1	104	72
250	22.5	10.5	12.8	116	72
200	25.0	10.5	12.9	123	68
150	27.5	10.5	14.0	111	62
100	30.0	11.5	16.2	93	67
70	31.3	12.0	18.1	90	71
50	31.3	13.0	20.0	90	82

FORECAST ERRORS (TROPICS)

LEVEL	GEOPOTENTIAL HEIGHT	U AND V COMPONENT	
		OLD	NEW
1000	14	4.0	1.9
850	15	4.0	2.9
700	17	4.5	3.2
500	22	6.5	3.7
400	27	8.0	4.5
300	30	8.0	4.5
250	32	9.0	4.3
200	32	10.0	4.0
150	35	13.0	3.6
100	38	13.0	3.3
70	41	11.0	3.5
50	48	8.0	3.6

TABLE 4 Revised observation errors in units of m for geopotential height Z and  $\text{ms}^{-1}$  for the wind components U and V.

LEVEL	RAWINSONDE, PIBAL, DROPSONDE			
	GEOPOTENTIAL		U, V	
	OLD	NEW	OLD	NEW
1000	7.0	7.0	1.8	1.4
850	8.0	7.5	1.8	2.2
700	8.6	8.5	2.4	2.4
500	12.1	11.0	3.8	2.8
400	14.9	13.7	4.7	3.4
300	18.8	15.2	5.9	3.4
250	25.4	16.0	5.9	3.2
200	27.7	16.1	5.9	3.0
150	32.4	17.5	5.5	2.7
100	39.4	19.1	4.9	2.5
70	50.3	20.5	4.9	2.5
50	59.3	24.0	3.9	2.7

	POLAR ORBITER SOUNDINGS		
	CLEAR	PARTLY CLOUDY	CLOUDY
1000	10.0	10.0	20.0
850	12.5	12.5	21.0
700	20.0	20.0	38.3
500	25.0	25.0	45.3
400	25.0	25.0	44.8
300	27.5	27.5	42.0
250	36.5	36.5	42.6
200	44.5	44.5	43.2
150	44.7	44.7	46.5
100	45.0	45.0	50.9
70	45.0	45.0	53.0
50	45.0	45.0	55.0

		OLD	NEW
CLOUD DRIFT WINDS			
HIGH LEVEL (U, V)		6.1-8.4	6.1
LOW LEVEL (U, V)		3.9-7.2	3.9
AIRCRAFT (U, V)		6.0	4.5
ASDAR/ACAR (U, V)		4.9	3.2
SFC BOGUS (Z)		7.0	32.0
SHIPS (Z)		7.0	7.0
	(U, V)	2.5	2.5
BUOYS (Z)		7.0	7.0
	(U, V)	2.5	2.5

total forecast error variance represents an upper bound on the observation error estimate. An examination of these minimum values reveals a latitude dependence for both height and wind components. However, since the present scheme does not permit latitude or station-dependent observation errors, the table has been constructed by averaging the minimum values over latitude. This number is quite close to the values carried by the ECMWF, particularly for the wind components (Thiebaut, personal communication).

For the aircraft wind entries, the values were based upon collocation studies and the somewhat subjective conclusion that inertial-based winds from aircraft are at least as accurate as rawinsonde winds. The entries for satellite cloud motion vectors recognize the result that current statistics of observation minus forecast values do not show any significant variation by producer. The primary problem with cloud motion vectors is the consistent speed bias shown by all high level vectors.

The value of observation error for surface pressure bogus observations was increased significantly. The assumed observation error for buoys and ships remain the same. This change is entirely subjective and will be re-evaluated at some future time.

The values of the satellite temperature sounding errors were left as above. We plan to improve those estimates as well as the method of assimilation during 1989.

### 2.3.3 Modified Quality Control

Presently each observation is subjected to two gross limit quality control checks in addition to those performed during preprocessing. First, the observational increment (data - first guess) is compared to a gross toss limit and dropped from the data base if the gross limit is exceeded. Second, the increment is compared to another limit and flagged as large if this limit is exceeded. After the gross limit checks are completed, a nearest neighbor (buddy check) is performed (see Section 2.2). During the buddy check an isolated observation is dropped from the data base if it has been flagged as large during the gross check, otherwise it is kept. The current limit denoting large isolated residuals has been increased in the new version of the GDAS. The major impact of this change will occur in the southern hemisphere data sparse regions causing more observations to be retained by the assimilation system.

In the current system, tropical high-level geopotential residuals between 20N and 20S and above 400 mb are required to be within 1 standard deviation (see Table 1) regardless of the quality mark. A minor modification was made to remove the abrupt change in criterion by using a linear blend of the tropical value and the quality dependent extratropical value in the region between 20 and 30 degrees latitude in both hemispheres.



#### 2.3.4 Interactive Clouds

Satellite-derived clouds have also been used in the evaluation of interactive clouds in the global spectral model. The clouds in the present model are computed only to modify the radiative fluxes, through the processes of reflection, scattering, absorption, and emission. Since the current model carries no liquid or frozen water, clouds must either be pre-specified or else be diagnosed from model-predicted variables. Prior to November 30, 1988, cloud amounts and heights were obtained from a zonally-averaged climatology, which changed only seasonally. Since the clouds were fixed functions of height and latitude, they could neither respond to different initial conditions, nor properly evolve during the forecast. The new clouds, however, are diagnosed from model variables and recalculated before each call to the radiation package.

The diagnosis of the clouds - both stratiform and convective - is done by techniques similar to those developed by Slingo (1987). The stratiform clouds exist in three domains (high, middle, and low). Within each of the three domains, the cloud top for each domain is taken to be coincident with the cloudiest layer within that domain. Usually the cloud is allowed to be only one layer thick, except that close to the surface, where model layers are thinnest, the clouds are required to be at least 90 mb thick. For low clouds to exist, there is an additional requirement that vertical motion be either upward or only slightly downward (less than 0.5 cm/sec.).

For convective clouds, bases and tops are calculated in the model's Kuo convective routine. The cloud cover, determined as a logarithmic function of the model's convective precipitation rate at a grid point, can extend through all three domains. For sufficiently strong and deep convection, the scheme can produce a dense anvil. It can be seen from Figs. 1a and 1b, that this parameterization is capable of giving a reasonable approximation to the observed cloud field.

#### 2.3.5 Results of a Parallel Test

The modifications to the analysis and to the assimilating model, described in the previous section and in Campana et al. (1989), were placed into the NMC/Development Division parallel GDAS on October 20, 1988. A sample consisting of the first 20 days in November was chosen to compare the differences between the parallel and operational systems. Table 5 shows the rms and mean differences between the proposed and operational systems for this 20 day period. As shown in the table, the major impact of these modifications has occurred at 100 mb. At this level, heights are much lower in the parallel system and temperatures are colder in all upper level regions, with the tropical area showing the

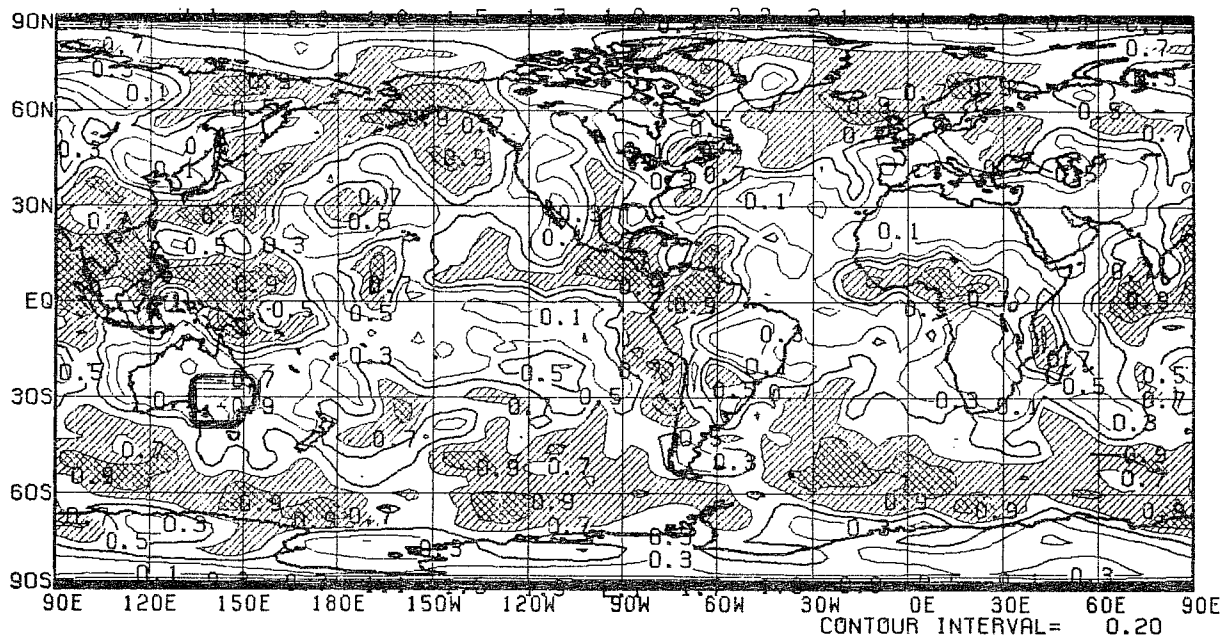


Fig. 1a. Observed total cloud fraction - Nimbus 7 (Hwang, et al., BAMS, 1988, p. 743.) 5 July 1979 - Equator crossing at 12Z. // greater than .7 - ▨ greater than .9.

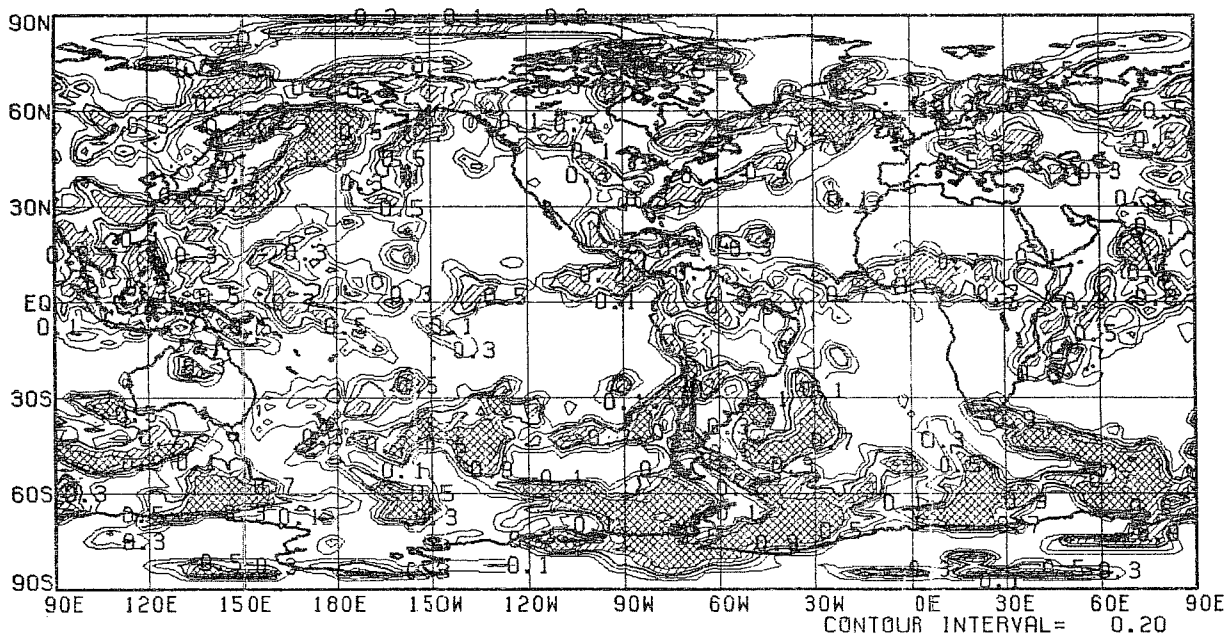


Fig. 1b. Model diagnosed total cloud fraction from MRF 24 hr data (valid at 00 UTC 5 July 1979). Total cloud computed by randomly overlapping high, mid, low cloud.

most impact. The parallel system is colder at upper levels in regions where rawinsonde observations are sparse because the warm bias has been reduced in the satellite temperature profiles.

Table 6 shows the difference between the two systems when compared to rawinsonde observations. Values are listed for the operational (before December 1988) and parallel system analysis and first guess fields. In most cases, the bias is closer to zero in the parallel system. However, the rms values indicate that the operational analysis "fits" the radiosonde observations better than the parallel while the six hour first guess fits the observations slightly closer in the parallel system. Evidently, the new ratio of observation errors to forecast errors has instructed the optimal interpolation analysis in the new system to rely more on the first guess values than was the case in the operational system.

The impact of these changes on the MRF forecasts is described in Campana et al. (1989). These changes plus those made to the numerical model have in most cases slightly improved the skill scores for medium range forecasts. However, the major improvement has occurred in the temperature and height field biases which are significantly reduced.

#### 2.4 Comparison of Physical and Statistical Retrievals

The retrieval process in use for many years at NESDIS was based on a statistical comparison of a large number of radiosonde reports with collocated TIROS Operational Vertical Sounder (TOVS) radiance measurements. Temperature profiles produced in this manner were, therefore, referred to as statistical retrievals. This technique served the meteorological community well over the years. However, this approach had the deficiency that it tended to not depart from mean conditions very far. The resulting retrievals generally underestimated gradients. In an attempt to alleviate this deficiency, NESDIS has recently developed an alternative technique -- the NESDIS TOVS Physical Retrieval System -- which utilizes a priori physical knowledge of the atmosphere and thereby substantially reduces the number of radiosonde reports needed for a statistical comparison. The temperature profiles produced by this procedure are referred to as physical retrievals.

The data impact studies described here were performed by first insuring that the parallel GDAS system exactly reproduced the operational GDAS results, then admitting the physical retrievals to the parallel GDAS analyses, while the statistical retrievals continued to be used in the operational GDAS. As a time saving measure, the parallel MRF forecasts were integrated only to 5 days instead of the operational length of 10.

TABLE 5

Analysis differences parallel system minus operational system for November 1 to 20, 1988.

GEOPOTENTIAL HEIGHT (m)							
LEVEL	NH		SH		TROPICAL		
	MEAN	RMS	MEAN	RMS	MEAN	RMS	
1000	0.5	3.8	1.4	4.5	-1.1	2.7	
850	0.0	3.4	0.6	3.1	-0.8	2.1	
500	-0.3	1.7	0.4	3.2	-1.5	2.8	
250	-1.3	2.3	-4.1	5.3	-3.3	4.2	
100	-9.1	14.8	-18.0	19.9	-25.6	28.7	

TEMPERATURE ( K )							
LEVEL	NH		SH		TROPICAL		
	MEAN	RMS	MEAN	RMS	MEAN	RMS	
1000	-0.2	0.5	-0.3	0.7	0.1	0.5	
850	0.0	0.2	-0.1	0.3	0.1	0.2	
500	0.0	0.1	0.0	0.1	0.0	0.1	
250	-0.2	0.3	-0.8	0.8	-0.4	0.4	
100	-0.2	0.4	-0.2	0.3	-0.6	0.7	

TABLE 6

Parallel and operational systems compared to radiosonde observations using the NH102 network.

	MEAN VALUES		RMS VALUES		MEAN VALUES		RMS VALUES	
	ANALYSIS	ANALYSIS	ANALYSIS	ANALYSIS	GUESS	GUESS	GUESS	GUESS
	OPL	PAR	OPL	PAR	OPL	PAR	OPL	PAR
850 MB								
Z	0.5	0.5	7.3	8.0	2.9	1.0	13.2	13.7
T	0.5	0.5	2.0	2.1	-0.2	-0.1	4.1	4.5
SPD	-0.5	-0.5	2.6	2.9	-0.4	-0.3	3.4	3.4
VECT	3.0	3.0	3.6	3.9	4.1	4.1	4.7	4.8
500 MB								
Z	0.4	0.0	10.1	10.6	-1.2	-1.9	17.4	17.1
T	0.2	0.2	1.2	1.2	-0.1	-0.2	1.4	1.4
SPD	-0.4	-0.5	3.1	3.1	-0.7	-0.7	4.0	4.0
VECT	3.4	3.5	4.1	4.1	4.7	4.6	5.5	5.4
250 MB								
Z	1.8	0.9	18.7	18.9	2.7	0.3	28.3	27.9
T	0.3	0.3	1.5	1.4	0.8	0.5	2.1	1.9
SPD	-0.5	-0.5	3.6	3.5	-1.0	-1.0	4.9	4.9
VECT	4.0	3.9	4.7	4.6	5.6	5.5	6.6	6.6
100 MB								
Z	4.6	0.9	32.8	31.4	6.6	-1.3	45.3	44.5
T	0.3	0.2	1.7	1.6	0.8	0.6	2.5	2.3
SPD	0.1	0.0	2.3	2.2	0.6	0.2	4.0	3.7
VECT	2.6	2.5	3.1	3.0	4.6	4.2	5.5	5.0

The first experiment began at 0000 UTC on September 11, 1987, and ended at 1800 UTC on October 1, 1987, for a total of 21 days, with each system producing its own analyses and forecasts from different first guesses. During the experiment, the number of non-TOVS observations available to the operational and parallel analyses was closely monitored and found to be identical at every individual analysis time during the 21 days.

The first impact study showed that the physical retrieval system performed generally better in the southern hemisphere, but slightly worse in the northern hemisphere, as illustrated in Table 7. In addition, the path C physical retrievals were found to have a significant cold bias. These results led us to conclude that the physical retrievals should not be used operationally at that time. Thereafter, a period of over 6 months ensued, during which NESDIS made various improvements to the physical retrieval system, after which a second data impact study was performed. During this 6-month period, several changes were made to the operational GDAS system as well. A second data impact study began at 0000 GMT on April 6, 1988 and ended at 1800 GMT on April 18, 1988. In this study, the physical retrieval system performed better in both hemispheres (Table 8), although there was less improvement in the southern hemisphere than in the first study. This may be due to the physical retrieval system performing relatively better in the winter hemisphere. The cold bias in the path C physical retrievals remained, although it was reduced in the northern hemisphere. The results of the second data impact study were sufficiently encouraging to justify operational use of temperature retrievals produced by the new method. This occurred on September 20, 1988.

### 3. CURRENT PROBLEMS WITH SATELLITE DATA

Clearly, the way that satellite data are being utilized in the GDAS is much less than optimal. For example, the accuracy of the 6 hour forecast is of the order of 1 K in the lower troposphere, while that of the satellite temperatures produced operationally is typically 3 to 4 K. Regional biases during the winter over the oceans east of the northern hemisphere continents are even larger (A. Hollingsworth, personal communication). Under these circumstances the best that can be hoped for is that the quality control system is sophisticated enough to delete the poor quality satellite data in order to avoid negative forecast impacts in the northern hemisphere. A few examples of negative impacts from satellite temperatures have even recently been noted in the southern hemisphere (J. Alpert, personal communication). While the above situation is probably the most serious, other problems are also contributing to the less-than-optimal utilization of the satellite data. These are briefly discussed here and include:

Table 7 Verification of 3 Day Forecasts from the first data impact study, September 11, 1987 - October 1, 1987

102 Northern Hemisphere Stations

	Mean Hgt. Error		Standard Deviation of Hgt. Error		RMS Vector Wind Error	
	Stat.	Phys.	Stat.	Phys.	Stat.	Phys.
850 hPa	- 0.1	- 0.5	34.3	35.0	7.3	7.3
500 hPa	-17.8	-18.5	44.8	44.8	8.8	8.8
250 hPa	-14.5	-16.0	64.2	64.0	13.5	13.7
100 hPa	-46.3	-47.4	55.4	56.4	6.6	6.7

110 North American Stations

	Mean Hgt. Error		Standard Deviation of Hgt. Error		RMS Vector Wind Error	
	Stat.	Phys.	Stat.	Phys.	Stat.	Phys.
850 hPa	- 6.0	- 7.0	26.2	26.4	6.5	6.5
500 hPa	-27.8	-29.0	35.9	36.6	8.3	8.4
250 hPa	-27.3	-28.2	58.3	59.5	14.9	15.0
100 hPa	-42.1	-42.5	41.8	43.5	7.6	7.8

31 Southern Hemisphere Stations

	Mean Hgt. Error		Standard Deviation of Hgt. Error		RMS Vector Wind Error	
	Stat.	Phys.	Stat.	Phys.	Stat.	Phys.
850 hPa	- 8.0	- 4.0	36.9	36.3	8.9	9.0
500 hPa	-24.3	-20.9	52.0	51.3	11.0	11.1
250 hPa	-10.4	- 3.4	71.7	70.6	16.3	16.3
100 hPa	-31.1	-23.4	66.0	64.6	10.5	10.3

Table 8

Verification of 3 Day Forecasts from the  
second data impact study, April 6, 1988 -  
April 18, 1988

## 102 Northern Hemisphere Stations

	Mean Hgt. Error		Standard Deviation of Hgt. Error		RMS Vector Wind Error	
	Stat.	Phys.	Stat.	Phys.	Stat.	Phys.
850 hPa	- 1.1	- 1.3	43.8	43.2	8.5	8.4
500 hPa	-24.2	-24.2	58.2	57.0	11.1	11.0
250 hPa	-24.0	-23.1	77.2	75.8	14.4	14.2
100 hPa	-49.3	-49.4	66.3	66.7	8.0	8.0

## 110 North American Stations

	Mean Hgt. Error		Standard Deviation of Hgt. Error		RMS Vector Wind Error	
	Stat.	Phys.	Stat.	Phys.	Stat.	Phys.
850 hPa	3.9	4.3	34.3	34.0	7.7	7.6
500 hPa	-22.1	-21.4	51.2	49.4	11.1	10.8
250 hPa	-14.8	-11.8	73.6	70.7	16.1	15.5
100 hPa	-35.9	-33.7	48.4	48.0	8.1	8.0

## 31 Southern Hemisphere Stations

	Mean Hgt. Error		Standard Deviation of Hgt. Error		RMS Vector Wind Error	
	Stat.	Phys.	Stat.	Phys.	Stat.	Phys.
850 hPa	- 0.4	- 1.3	29.1	28.1	7.5	7.6
500 hPa	-14.4	-15.8	38.8	40.7	9.7	9.5
250 hPa	- 4.1	- 5.6	58.7	59.3	16.4	15.6
100 hPa	- 0.0	1.6	53.0	51.1	10.1	9.8

1) The analysis of satellite height needs to be replaced with an analysis of thickness. Originally, analyzing satellite heights seemed to be an advantage because of the oscillation in the vertical between warm and cold biases which permitted some cancellation in the mid and upper troposphere. However, as the accuracy of the model 6 hour forecast has continued to improve, the lower tropospheric satellite temperature error has become a significant source of error in the mid and upper troposphere through the integration to produce height profiles. Anchoring the satellite height profiles in a consistent manner between land and ocean is also a problem. In the near future, we plan to develop an analysis of satellite thickness once the development of a model-level-based analysis is completed (currently the analysis is performed on mandatory pressure levels).

2) The sat-sat error correlation statistics are outdated. The present sat-sat correlation statistics used in the optimum interpolation analysis are based on a study by Schlatter (1981) which were appropriate for the polar orbiting satellites in the early 1980's in which statistical regression was used to produce the retrievals (Smith and Woolf, 1976). More recently, with the implementation of a physical retrieval scheme (Fleming et al., 1986, 1988) at NESDIS, the sat-sat correlation statistics need to be revised. For this purpose, a collaborative effort between NESDIS and NMC is underway using currently produced sounding data.

3) The quality control of SATEMS is not adequate. As mentioned earlier, this is a serious deficiency in the NMC system, particularly with respect to the occasional negative forecast impacts obtained from satellite data. It should be noted that other centers have also obtained negative forecasts impacts from satellite data as well (e.g., ECMWF, GLA). A major effort is now underway to revise the entire quality control system at NMC incorporating the ideas of Gandin (1988) on complex quality control. With this approach, several checks, which are observing-system-dependent, will be made in parallel, rather than serially. The final decision of whether to accept or reject a particular piece of data will be based on all of the available information.

4) The negative bias in the high-level cloud-track winds (CTW's) is particularly serious in strong wind situations in the northern hemisphere (i.e. in the subtropical jet). There are undoubtedly several sources for this error. In the near term, we plan to conduct an experiment in which the wind direction from the CTW's is combined with the wind speed from the 6 hour forecast for those situations in which the wind speed of the model forecast is significantly stronger than that of the nearby CTW's.

In the longer-term the CO<sub>2</sub> slicing technique (Merrill, 1989), seems promising. An evaluation of data produced at NESDIS using that approach is planned, as well as tests with



15 min data (e.g., Peslen, 1980) compared to the presently operational 30 min data. In addition, in order to improve the quality of the data in the southern hemisphere, NMC has begun providing to NESDIS 12 h forecasts for use in CTW production and height assignment. Previously, NESDIS has used a climatological height assignment for the high-level winds in the southern hemisphere (T. Stewart, personal communication).

#### 4. DEVELOPMENT OF AN INTERACTIVE RETRIEVAL SYSTEM

NMC and NESDIS have recently initiated a collaborative effort to develop an interactive analysis/forecast/retrieval system to optimize the use of satellite data in the assimilation. Previous work in this area at the NASA/Goddard Space Flight Center by J. Susskind and collaborators has been particularly promising. In addition to temperature profiles and thick-layer precipitable water estimates, a wide range of geophysical parameters (e.g., land and sea surface temperature, ice and snow extent, cloud top pressure and amount, and estimates of outgoing long wave radiation, soil moisture, total ozone, precipitation, and a vegetation index) can also be produced. A particularly strong point with the interactive approach is that the above parameters are obtained in a way which is consistent with the mass and wind fields in the assimilation because the 6 hour forecast from the assimilation is used as the first guess for the retrievals. Also, producing and using temperature retrievals interactively during the assimilation, based on the NASA experience, should result in a more accurate 6 hour forecast. Since the non-retrievable components of the soundings are obtained from the first guess rather than from climatology, this method should eliminate many, if not most of the negative impacts on medium-range forecasts.

A suitable satellite retrieval scheme for this purpose would likely be a combination of those developed at NESDIS (e.g., Fleming et al., 1986b, 1988; McMillin, 1986) and at NASA (Susskind et al., 1984). In the future, we plan to conduct parallel tests of the different retrieval approaches and combine the strong points of each in order to develop a state-of-the-art system for retrieving and utilizing satellite data.

#### 5. OTHER DEVELOPMENT EFFORTS

There are a variety of other research activities at NMC utilizing satellite data which are discussed below.

##### 5.1 Surface Winds

In anticipation of the arrival of scatterometer oceanic surface wind data from European, Japanese and U.S. satellites in the earlier 1990's, we have conducted one week

assimilation experiments using scatterometer winds from SEASAT in the current NMC operational GDAS. The SEASAT scatterometer wind data set used in this study was provided by R. Atlas of GLA/NASA and carefully edited by JPL. Two sets of assimilation experiments were conducted, one with scatterometer winds, the other without. In the assimilation experiments, the scatterometer winds were treated as if they were ship winds, starting at 0000 UTC September 7, 1978 and ending at 0000 UTC September 14, 1978.

In view of the fact that the currently available DMSP Special Sensor Microwave Imager (SSM/I) can measure ocean surface wind speed, and this data set will soon be operationally available at NMC, we have begun working with that data also. Recently, a set of SSM/I wind speed data were provided to us by R. Atlas. Unlike the SEASAT scatterometer data, the SSM/I data set contains only wind speed information. As a first attempt to use the data in the NMC GDAS, the directions for the SSM/I wind speed data are taken directly from those of the 1000 mb wind analyses.

Three days of assimilation were conducted with one experiment including the SSM/I wind speed data and the other without, starting at 0000 UTC August 14, 1987 and ending on at 0000 UTC August 17, 1987.

Figure 2 shows the differences in the 1000 mb height (top) and wind (bottom) fields after 7 days of assimilation. Large differences occur in the southern hemisphere where conventional data are sparse, with little impact in the northern hemisphere where other sources of data are more abundant. The largest differences are seen to be in excess of 300 meters at 1000 mb with accompanying vector wind differences of greater than 20 m/sec in the south western Australia region. These differences become smaller in the upper troposphere, and as expected, eventually diminish beyond 250 mb (not shown). This is in agreement with the results of a recent data assimilation study by Anderson et al., (1987), which utilized the SEASAT scatterometer wind data in the ECMWF global data assimilation system.

Figure 3 shows the differences with and without SSM/I wind speed data for the 1000 mb height (top) and wind analysis (bottom) after three days of assimilation. Similar to the findings in the scatterometer experiments, we see that including the SSM/I wind speed data leads to large differences in the southern hemisphere, and a very small impact in the northern hemisphere. Differences are as large as 200 meters in the height and 15 m/sec in the wind fields in the southern hemisphere.

Tables 9 and 10 show that the SEASAT scatterometer winds after 7 days of assimilation have had a clear positive impact in the Southern Hemisphere by reducing the error of the first guess. The number of rawinsondes rejected in the quality control is also reduced because of the better agreement with the first guess. In the Northern Hemisphere the overall impact was negligible. A similar comparison

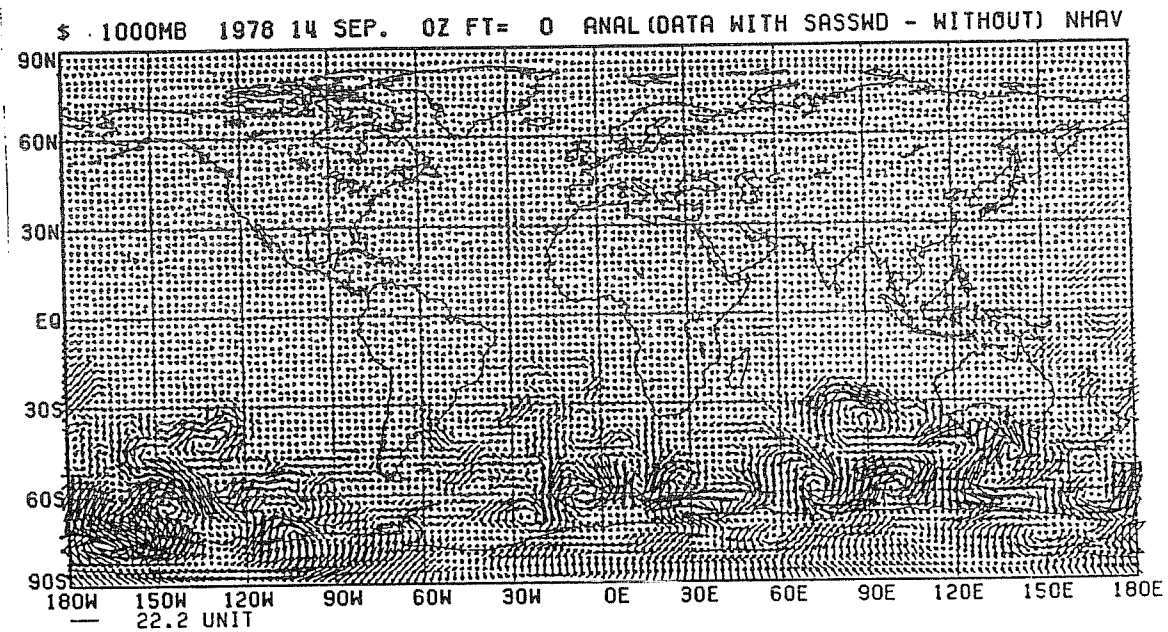
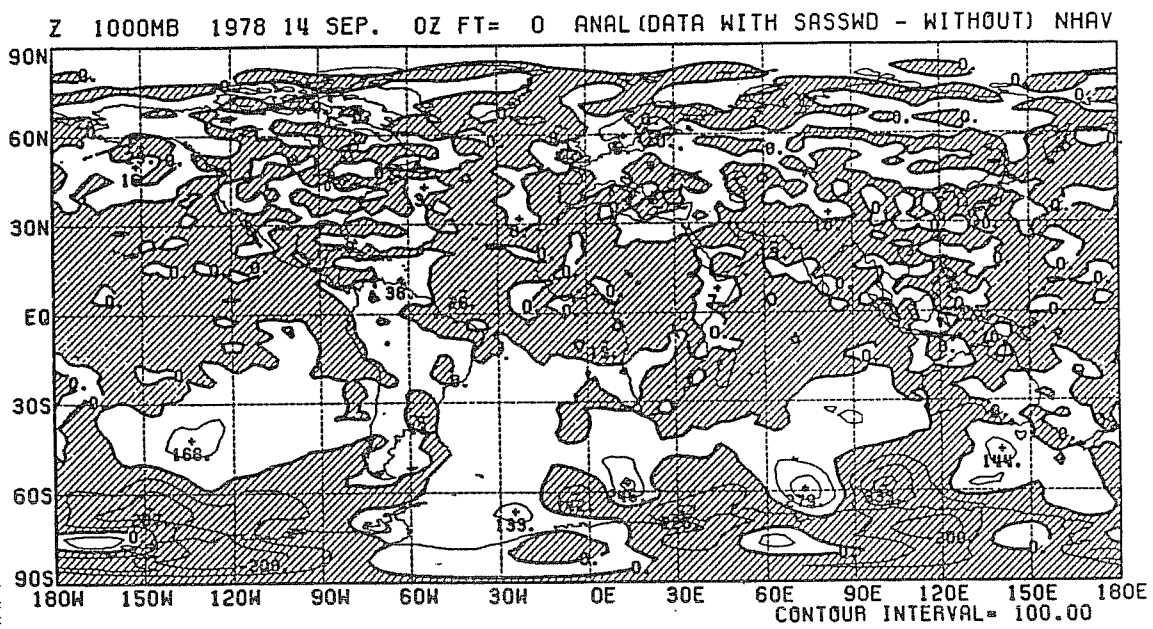


Fig. 2. Differences of Analyses after seven days of data assimilation between the experiment with SEASAT Scatterometer winds and that without for 1000 mb heights (top), and 1000 mb vector winds (bottom).

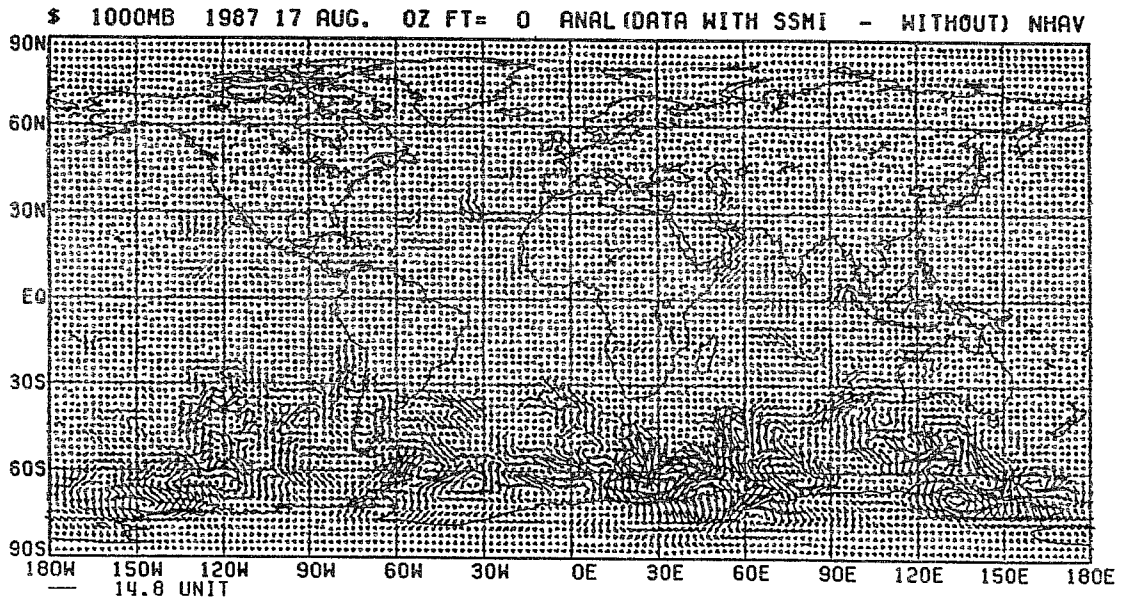
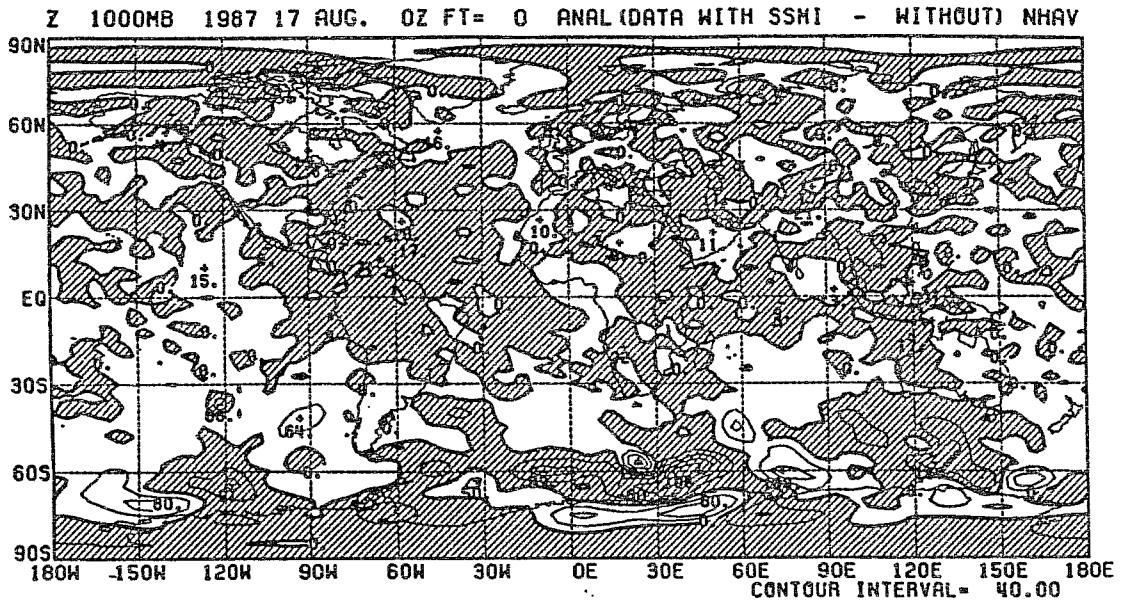


Fig. 3. Differences of Analyses after three days of data assimilation between the experiment with the DMSP SSM/I wind speed data and that without for 1000 mb heights (top), and 1000 mb vector winds (bottom).

Table 9: Standard deviation of the fit of the first guess heights (m), and u and v wind components (m/s) to the Southern Hemisphere radiosonde data for the experiment including SEASAT scatterometer winds (valid 9/14/00Z/1978). The number inside the bracket indicates the number of radiosondes used in the analysis.

		1000 mb	700 mb	500 mb	250 mb
Z	90S-60S	(10) 47.37	48.12	63.03	86.91
	60S-30S	(24) 20.67	21.35	40.48	56.80
	30S-0	(31) 27.50	16.20	15.45	27.23
U	90S-60S	( 1) 0	9.73	8.79	14.53
	60S-30S	( 4) 1.71	3.93	5.23	8.84
	30S-0	(12) 2.83	4.55	4.79	7.43
V	90S-60S	( 1) 0	7.71	8.10	13.15
	60S-30S	( 4) 2.09	4.93	6.58	13.56
	30S-0S	(12) 1.37	4.31	6.27	9.28

Table 10: As in Table 9, except for the experiment without SEASAT scatterometer winds.

		1000 mb	700 mb	500 mb	250 mb
Z	90S-60S	( 7) 58.50	56.87	88.18	154.00
	60S-30S	(24) 18.15	17.45	41.87	62.21
	30S-0	(31) 24.19	17.51	17.97	30.01
U	90S-60S	( 1) 0	10.30	9.83	13.15
	60S-30S	( 4) 2.78	4.03	6.42	9.22
	30S-0	(12) 2.74	4.31	5.55	8.45
V	90S-60S	( 1) 0	9.09	11.14	15.34
	60S-30S	( 4) 3.48	6.29	7.42	12.60
	30S-0S	(12) 1.66	4.20	5.68	9.30

after 3 days of SSM/I data assimilation (not shown) indicates a negligible impact in both hemispheres.

Future plans include developing a analysis scheme which is stability dependent with respect to the vertical influence of oceanic surface wind data.

## 5.2 Altimeter Data

A series of experiments at NMC have shown the potential for improvement in wave forecasts if wave and wind data are available in near real time. Significant wave height (SWH) and wind speeds from the SEASAT altimeter were used to produce initial wave fields for the wave forecasts (Esteva 1988, 1989).

Figure 4 shows the percentage improvement achieved in mean absolute error in the SWH forecasts at 6, 12, 18, and 24 hours for each of the 10 days of the experiments. The solid line denotes improvements when SWH data only were used; the dashed line the improvement with both SWH and wind speed data. The bottom panel shows improvements for the 30, 36, 42, and 48 hour forecasts. Addition of the wind information has little effect after 24 hours.

Although one single polar orbiting satellite flying an altimeter provides limited coverage of the global oceans and limited information about waves and winds, an average improvement of approximately 12% was achieved in the second experiment. This would indicate that a larger coverage and/or a more complete description of both wind and wave fields would result in larger improvements. Thus, near real time data from instruments such as the Synthetic Aperture Radar (SAR), providing directional wave spectra, and scatterometers (e.g., ERS-1, NSCAT, SCATT-2) providing both wind speed and direction would be very valuable.

## 5.3 Sea Surface Temperature Analysis

Three sea surface temperature (SST) analyses have been routinely produced at NMC by the Climate Analysis Center and the Ocean Products Center for the Tropical Ocean Global Atmosphere (TOGA) program. The three analyses are: an in situ analysis (ship and buoy), a satellite, and a blended analysis. All analyses are computed using SST anomalies, i.e., the monthly SST climatology is subtracted from the SST values. (The climatology was derived by Reynolds and Roberts (1987) from in situ, satellite and sea ice data. It is available as monthly fields on a 2 degree grid.) The blended analysis is the final TOGA product. In the blend, the in situ analysis is used to define internal boundary conditions in regions of frequent in situ observations. In the remaining regions, the solution is obtained using Poisson's equation. There, the Laplacian of the satellite analysis is used to force the Poisson solution. The Poisson method was chosen primarily because it objectively

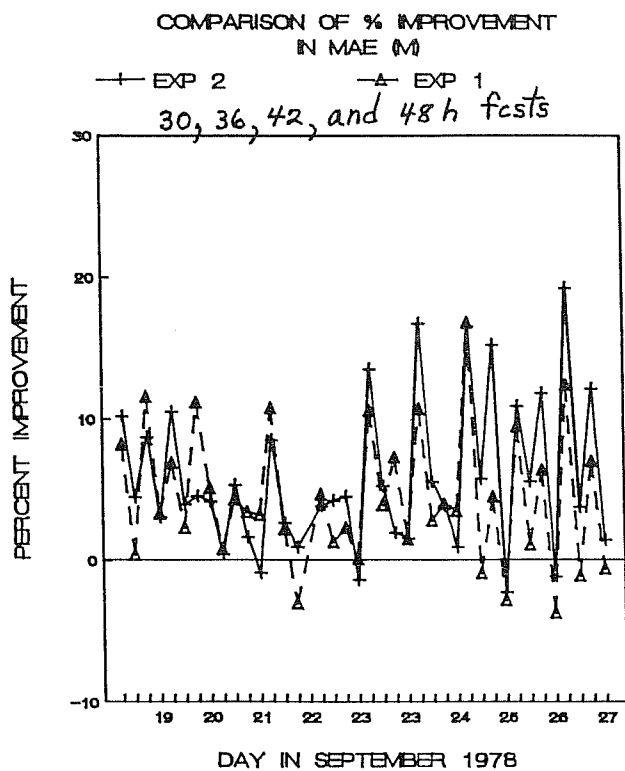
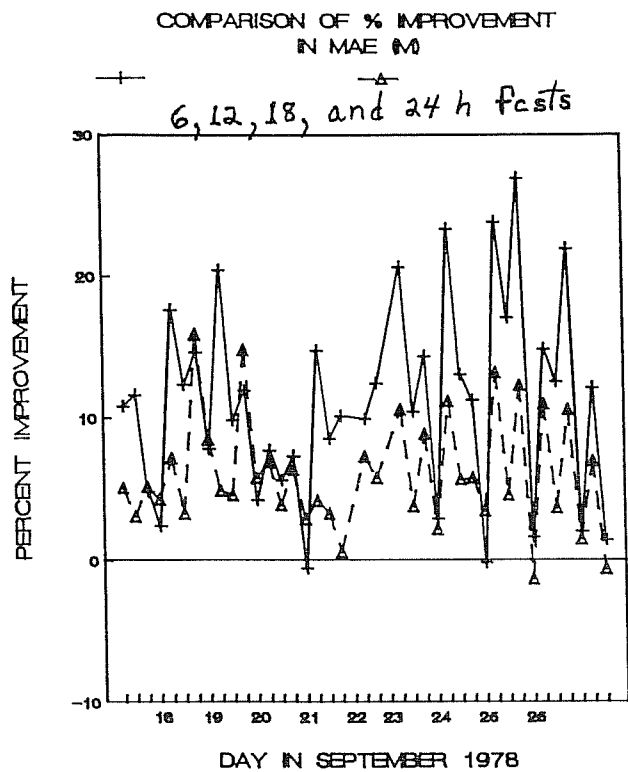


Fig.4. Percent improvement in mean absolute error (MAE) of significant wave height (SWH) forecasts using SWH data only (dashed line) and SWH and wind speed data (solid line). See text for details.

eliminates both the bias and large scale gradients of the satellite field between the internal boundary points. Complete details of the analysis techniques can be found in Reynolds (1988).

During the past 18 months, work has been completed on three archives for the SST product. Two archives, the in situ and satellite (see McClain et al., 1985, for details) are improved from earlier versions. The sea ice cover archive is new.

The sea ice cover archive was developed by K. Campana (NMC/Development Division). It consists of a weekly 2 degree gridded field of snow and ice cover. The fields are derived from satellite ice cover data from the U.S. Navy/NOAA Joint Ice Center and satellite snow cover (northern hemisphere, only) data from NESDIS. The gridded fields begin with the first week in January 1988.

Effective January 1989, the blended analysis was modified to use the sea ice archive. Regions which were covered by sea ice for more than half of the month were set to -1.8 degrees C (the freezing point of sea water with salinity of 35 parts per thousand). The blended technique uses Poisson's equation to objectively eliminate biases in the satellite field. However, in order to make the solution a mathematically well-posed problem, SSTs must be specified at external boundaries which completely enclose the interior region. Before the sea ice cover was available, the external boundary conditions (especially in the southern hemisphere) were often determined by the satellite analysis. The use of satellite data in this case permits possible satellite biases to enter the analysis locally. The availability of the sea ice cover allows the external boundary conditions to be independent of satellite SST information. An example of the mean blended field for February 1989 using the sea ice data is shown in Figure 5. The -1 degrees C contour closely parallels the ice covered regions (indicated by stippling). Figure 6 shows the difference between the blend with and without the ice information. As expected, the analysis with ice is colder than the analysis without ice at high latitudes. Significant differences (absolute SSTs greater than 0.5 degrees C) are confined to regions north of 50N and south of 50S.

The in situ and satellite analyses have been modified to use the improved in situ and satellite archives. Both the in situ and satellite analyses can now be computed for any period from 1 to 36 days. The blended analysis is now being modified to use the modified in situ and satellite analyses. Once these changes are complete, careful comparison of the old and new analyses will be carried out for several months before the new blended analysis becomes the official TOGA product. It is expected that there will be little change between the old and new monthly fields. The major advantage of the new system is that the blended field can be computed for any period from 1 to 36 days.



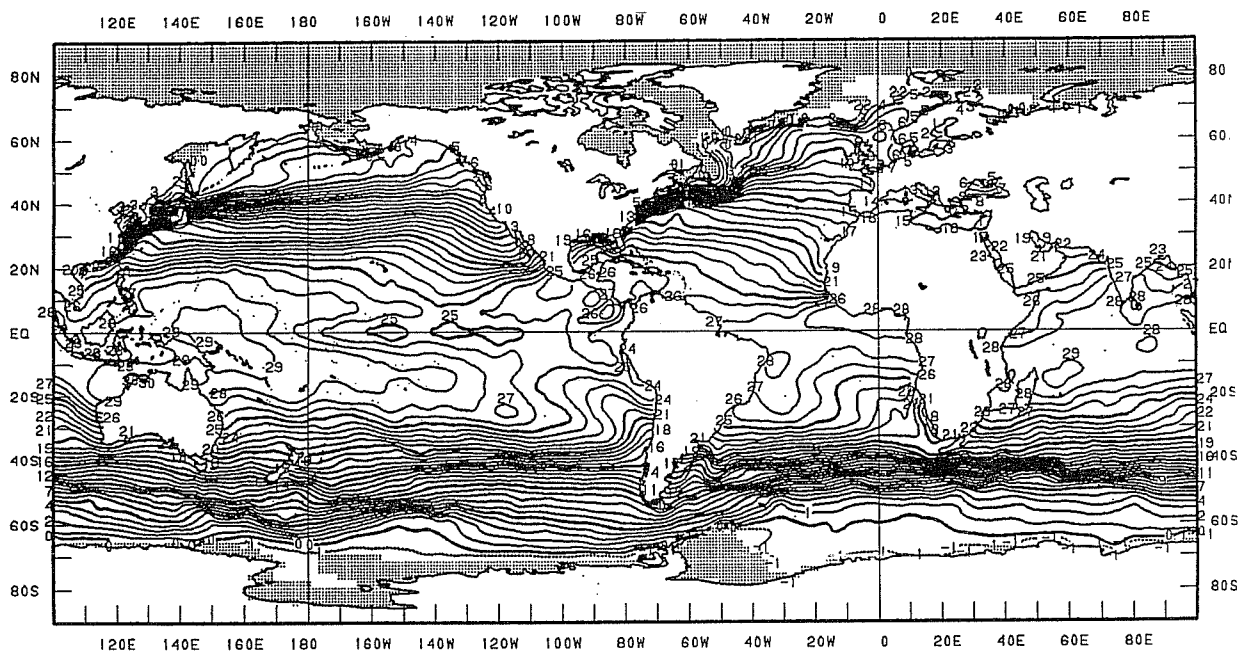


Fig. 5. The blended mean SST field using sea ice cover for February 1989. The contour interval is  $1^{\circ}\text{C}$ . The ice covered regions are indicated by stippling.

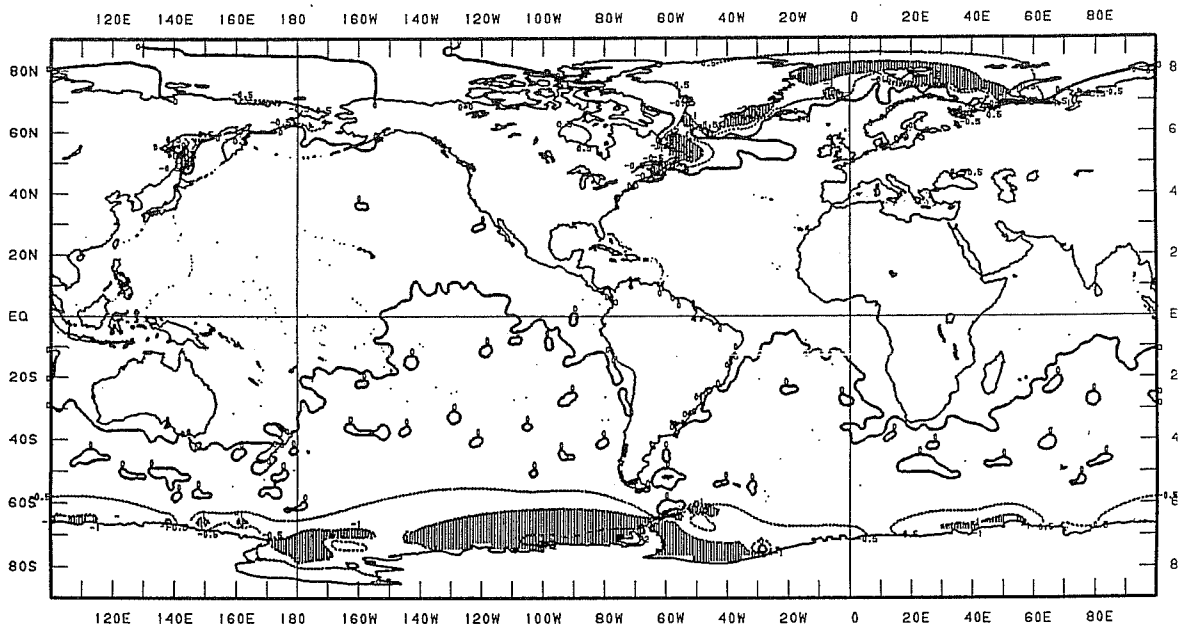


Fig. 6. The difference between the blended SST analysis with and without sea ice (ice - no ice) for February 1989. The contour interval is  $1^{\circ}\text{C}$ , except there is an extra contour at  $-0.5^{\circ}\text{C}$ . Positive contours are solid lines; negative contours are dashed. The  $0^{\circ}\text{C}$  contour is a heavy solid line. Shading indicates regions where the difference is less than  $-1^{\circ}\text{C}$ .

In all versions of the blended analysis, the in situ analysis provides internal boundary conditions which permit the automatic adjustment of possible satellite biases for each analysis period. This method is used because satellite biases are not constant but vary with space and time. An example of the satellite biases and the automatic adjustment of the blend is shown in Figure 7. This automatic adjustment of satellite biases is the major advantage of the blended technique. To provide accurate in situ internal boundary points, the in situ analysis is smoothed by a median filter which degrades the resolution to approximately 6 degrees. This affects the resolution of the blended product. The degradation of spatial resolution is the major disadvantage of the blended technique.

During the next year, we plan to investigate the use of an OI technique to analyze the global SST field with finer temporal and spatial resolution. A regional higher resolution SST OI analysis has been developed by A. Leetmaa (NMC/Climate Analysis Center) using a first guess generated by a tropical ocean model. We plan to expand this method to the global domain. The OI scheme must use careful quality controlled SST data because the higher resolution results in fewer observations per grid interval and because the OI doesn't automatically eliminate satellite biases. The improved in situ and satellite archives will facilitate the needed higher quality control. Once the global OI technique has been developed, the OI analysis will be carefully compared with the blend to show the advantages and disadvantages of the two methods.

#### 5.4 Global Snow/Sea Ice Extent and Vegetation Index

The weekly Navy/NOAA Joint Ice Center global sea-ice boundary analysis and the weekly NESDIS northern hemisphere snow cover analysis are currently available based on satellite data. Algorithms have been developed to incorporate this information into the Medium-Range Model to improve the snow and sea-ice initial state. Recently, a T80 10-day forecast was made using the data set. Comparison with the operational forecast shows that there are significant improvements in the lower atmospheric thermal structure in regions where the analyzed and (operational) climatological snow and sea-ice are quite different. There is also evidence of positive impact on the systematic error of the MRF in the Arctic region based on forecast days 6 to 10 of the 1000 mb and 500 mb height field (see Figure 8). We are planning to test operationally the inclusion of the data set during 1989.

Vegetation index data measured from satellite have been available for the past year. The weekly vegetation index data suffer from contamination due to persistent cloud cover. The vegetation index data over the Amazon region, for instance, are often lower than over North America. It is not clear whether the model forecast will be sensitive to the error in the satellite measurements. We plan to conduct

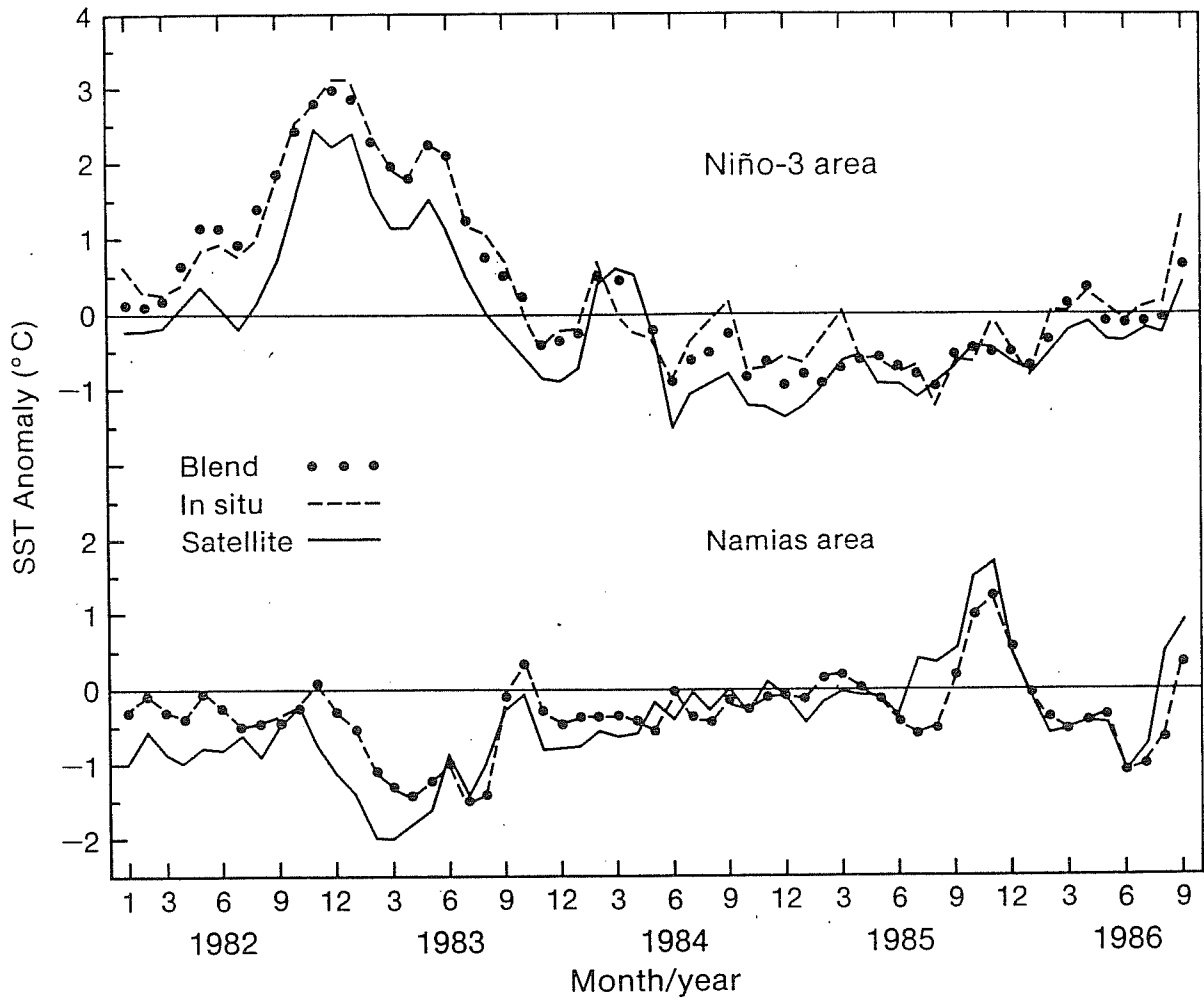


Fig. 7. Time series in in situ (dashed line) and satellite (solid line) SST anomalies for January 1982 to September 1986. The blended values (see text) are dotted. The Pacific regions are Niño 3 ( $5^{\circ}\text{S}$ - $5^{\circ}\text{N}$ ,  $90^{\circ}\text{W}$ - $150^{\circ}\text{W}$ ) and Namias ( $30^{\circ}\text{N}$ - $50^{\circ}\text{N}$ ,  $150^{\circ}\text{W}$ - $165^{\circ}\text{W}$ ).

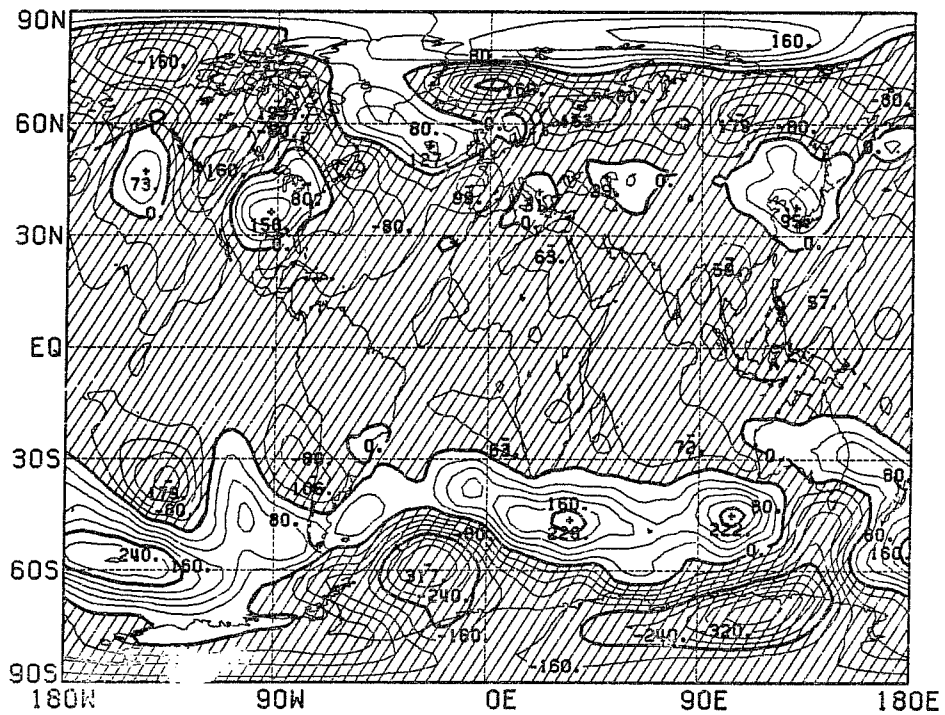
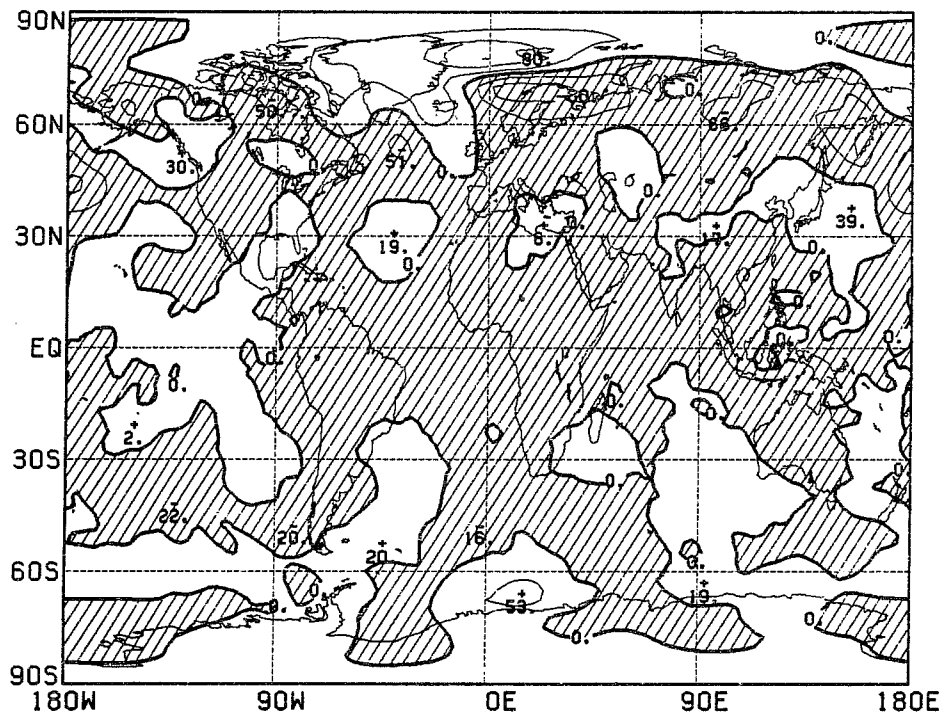


Fig. 8. The 500 mb height difference (operational-snow experiment), shown at the top, for the 5 day mean T80 forecast from 00Z 15 May 1988. Contour interval is 40 m and negative values are shaded. The operational-verification differences are shown at the bottom.

a test during 1989 to determine if the weekly vegetation index data can be incorporated into the medium-range forecast model.

## 5.5 Satellite-Derived Cloud Verification

NMC has a number of planned uses of satellite data for the improvement of the cloud parameterization schemes in its model. Currently, discussions are occurring between NMC and NESDIS which will result in "real-time" gridded cloud and radiation budget databases for operational, as well as, future versions of the models.

Cloud and radiative flux observations will be used to validate the cloud parameterizations, either by providing a general characterization of observed cloud fields or by permitting cloud point-verifications. Any deficiencies in the schemes will become evident (e.g., we know oceanic stratus is underestimated) and more complete tuning of parameters in the parameterizations (e.g. critical relative humidity) will be made. There are also plans to compute "effective" cloud radiative properties (e.g. reflectivity) from a "fit" of model-computed top of the atmosphere radiative fluxes to observations. Thus, the constant value of the properties, that are currently used with each cloud type, will be replaced with more realistic values.

A side-benefit of this work will be the potential discovery of deficiencies in other model processes; deficiencies which might be particularly evident in the modeled clouds. For example, errors in the vertical placement of low cloud-tops would suggest problems with vertical diffusion, surface evaporation, etc. Errors in tropical clouds could "implicate" model convective processes. Finally, in the future we plan to investigate the usefulness of cloud observations as initial data for the models. These observations could empirically provide relative humidity values in data sparse regions (needed for the current model-diagnosed cloud scheme) or provide initial estimates of cloud-water (needed for a future cloud-water variable).

## 6. ACKNOWLEDGMENTS

Several of our colleagues also contributed substantially to the work reported here including: B. Ballish, P. Caplan, J. Daniels, H. Fleming, L. Gandin, M. Goldberg, B. Katz, M. Kanamitsu, R. Petersen, J. Sela, and J. Thieboux.

## 7. REFERENCES

Campana, K., P. Caplan, and J. Sela, 1989: Changes to the global forecast model on November 30, 1988. NWS Technical Procedures Bulletin No. 384, NWS, Camp Springs, MD., in press.

Esteva, D. R., 1988: Evaluation of preliminary experiments assimilating SEASAT significant wave heights into a spectral wave model, J. of Geophys. Res., 93, C11, in press.

Esteva, D. C., 1989: Improving global wave forecasts incorporating altimeter data. To appear in Preprints Second International Workshop on Wave Hindcasting, Vancouver, Canada.

Fleming, H. E., M. D. Goldberg, and D. S. Crosby, 1986b: minimum variance simultaneous retrieval of temperature and water vapor from satellite radiance measurements. Preprints Second Conference on Satellite Meteorology/Remote Sensing and Applications, 13-16 May, Williamsburg, VA, Amer. Meteor. Soc., Boston, pp. 20-23.

Fleming, H. E., M. D. Goldberg, and D. S. Crosby, 1988: Operational implementation of the minimum variance simultaneous retrieval method. Preprints Third Conference on Satellite Meteorology and Oceanography, 31 January - 5 February, Anaheim, CA pp. 16-19.

Gandin, L. S., 1988: Complex quality control of meteorology observations. Mon. Wea. Rev., 116, 1137-1156.

McClain, E. P., W. G. Pichel and C. C. Walton, 1985: Comparative performance of AVHRR-based multichannel sea surface temperature. J. Geophys. Res., 90, 11587-11601.

McMillin, L. M., 1986b: The use of classification procedures to improve the accuracy of satellite soundings of temperature and moisture. Preprints Second Conf. on Satellite Meteorology/Remote Sensing and Applications, 13-16 May 1986, Williamsburg, VA. Amer. Meteor. Soc., Boston, 1-4.

Merrill, R. T., 1989: Advances in the automated production of wind estimates from geostationary satellite imagery. Preprints Fourth Conf. on Satellite Meteorology, San Diego, Amer. Meteor. Soc., Boston, in press.

Peslen, C. A., 1980: Short-interval SMS wind vector determinations for a severe local storm area. Mon. Wea. Rev., 107, 1407-1418.

Reynolds, R. W., and L. Roberts, 1987: A global sea surface temperature climatology from in situ, satellite and ice data. Tropical Ocean-Atmosphere Newsletter, 37, 15-17.

Reynolds, R. W., 1988: A real-time global sea surface temperature analysis. J. Climate, 1, 75-86.

Schlatter, T., 1981: An assessment of operational TIROS-N temperature retrievals over the United States. Mon. Wea. Rev., 109, 110-119.

Slingo, J. M. 1987: The development and verification of a cloud prediction scheme for the ECMWF model. Quart. J. R. Meteor. Soc., 113, 899-927.

Smith, W. L., and H. M. Woolf, 1976: The use of eigenvectors of statistical covariance matrices for interpreting satellite sounding radiometer observations. J. Atmos. Sci., 33, 1127-1140.

Susskind, J., J. Rosenfield, D. Reuter, and M. T. Chahine, 1984: Remote sensing of weather and climate parameters from HIRS2/MSU on TIROS-N. J. Geophys. Res., 89D, 4677-4697.